Asian Journal of Nanoscience and Materials 4 (2021) 229-239

Asian Journal of Nanoscience and Materials

Journal homepage: www.ajnanomat.com

Original Research Article

Toxicity testing of indocyanine green and fluorodeoxyglucose conjugated iron oxide nanoparticles with and without exposure to a magnetic field

Perihan Unak[a,*], Rachel Hepton[b], Max Harper[c], Volkan Yasakci[a], Gillian Pearce[c], Steve Russell[b], Omer Aras[d], Oguz Akin[d], Julian Wong[e]

[a] *Ege University, Institute of Nuclear Sciences, Department of Nuclear Applications, Bornova Izmir, 35100, Turkey*

[b] *Aston University, School of Life and Health Sciences, Aston Triangle, Birmingham, B4 7ET, United Kingdom*

[c] *Aston University, School of Engineering and Applied Sciences, Aston Triangle, Birmingham, B4 7ET, United Kingdom*

[d] *Memorial Sloan Kettering Cancer Centre, Department of Radiology, New York, USA*

[e] *University Hospital Singapore, Cardiothoracic and Vascular Surgery Department, Singapore*

ARTICLE INFORMATION

Received: 28 January 2021
Received in revised: 25 March 2021
Accepted: 28 March 2021
Available online: 27 May 2021

DOI: 1026655/AJNANOMAT.2021.3.5

KEYWORDS

Fluorodeoxyglucose
Indocyanine green
Iron oxide nanoparticles
Magnetic effect
NIC-H7272 cells

ABSTRACT

Iron nanoparticles (MNPs) are known to induce membrane damage and apoptosis of cancer cells. In our study we determined whether FDG coupled with iron oxide magnetic nanoparticles can exert the same destructive effect on cancer cells. This research study presents data involving NIC-H727 human lung, bronchus epithelial cells exposed to conjugated fluorodeoxyglucose conjugated with iron-oxide magnetic nanoparticles and indocyanine green (ICG) dye (FDG-MNP-ICG), with and without the application of a magnetic field. Cell viability inferred from MTT assay revealed that FDG-MNPs had no significant toxicity towards noncancerous NIC-H727 human lung, bronchus epithelial cells. However, percentage cell death was much higher using a magnetic field, for the concentration of FDG-MNP-ICC used in our experiments. Magnetic field was able to destroy cells containing MNPs, while MNPs alone had significantly lower effects. Additionally, MNPs alone in these low concentrations had less adverse effects on healthy (non-target) cells.

Corresponding author, email: perihan.unak@gmail.com (P. Unak).
Tel.: 90 5365131806.

Graphical Abstract

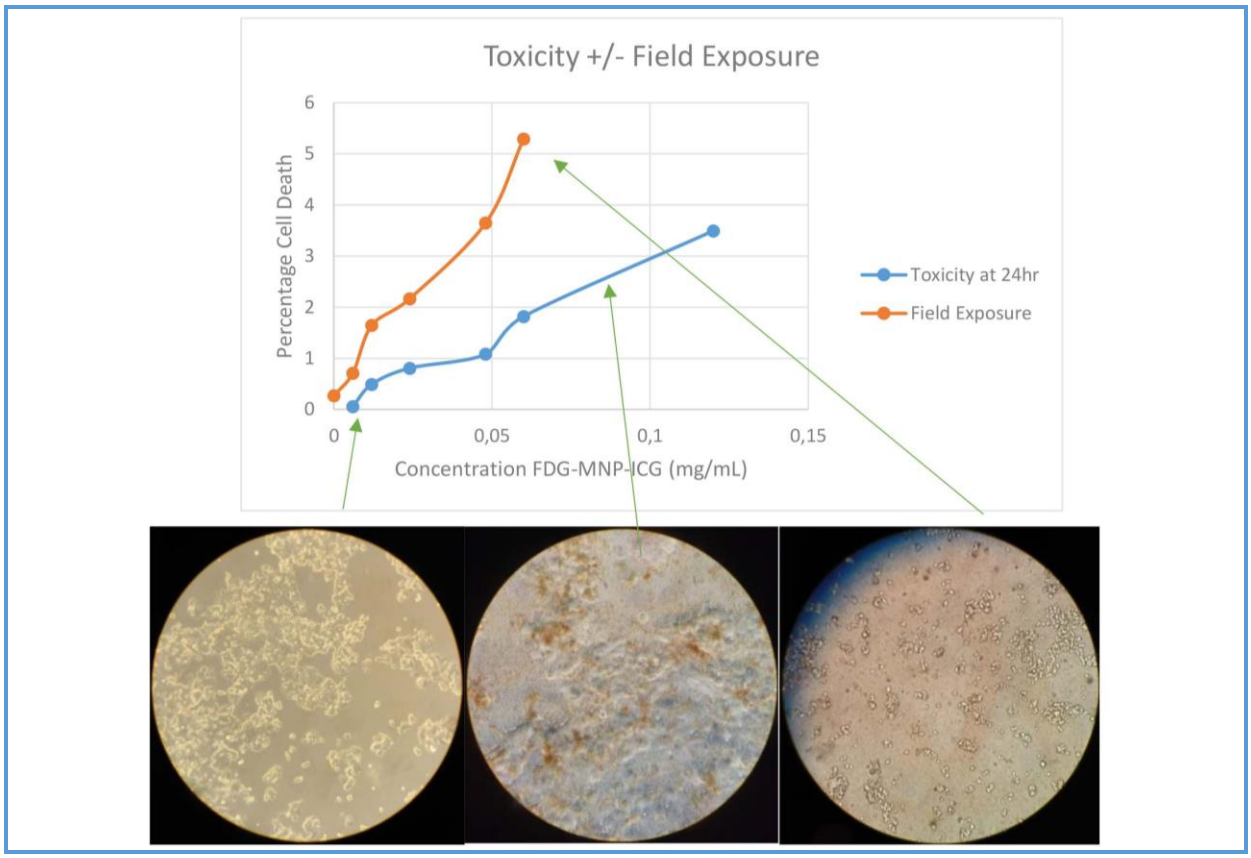

Introduction

The number of cancer cases world-wide has been continuously increasing [1–4]. For decades, classic treatments, including chemotherapy and radiotherapy constituted the main types of therapies used. However, some of these established cancer treatments revealed side-effects and problems with cancer resistance to chemotherapy drugs may develop in some instances. Furthermore, these drugs are costly to develop and, in many instances, take several years to develop and test before being used clinically. There is also the additional problem that not all cancers are responsive to radiotherapy or to cancer drugs. The majority of the anti-cancer drugs are hydrophobic with poor solubility, which may reduce the bioavailability. The effectiveness is brought out by enclosing them within some hydrophilic NPs to exert their therapeutic response [5]. It is recommended that MNPs maintain tolerable hydrophilicity with less than 100 nm in size and coating helps to bypass rapid clearance by reticuloendothelial system (RES) [6]. The magnetic particles are largely maintained at the target site and may be incorporated by the endothelial cells of the target tissue when the magnetic forces surpass the linear blood flow rates in arteries (10 $cm.s^{-1}$) or capillaries (0.05 $cm.s^{-1}$). For that reason, application the utilization of nanoparticles supports the transport though the capillary systems of organs and tissues avoiding vessel embolism [7]. These advancements in magnetic nanoparticles (MNPs) technology, has helped overcome many difficulties in the diagnosis and treatment of lung cancer. More recently new

potential treatments have included the use of new materials based on iron oxide magnetic nanoparticles (MNPs) [8–12]. MNPs have contrast property at MRI, besides they have potential for magnetic hyperthermia therefore they have theranostic potential [13, 14]. As early as 1984, hyperthermia together with MNPs was being used in cancer treatment [15] and this type of research has continued over the decades [16], together with investigations of the toxic effects of magnetic nanoparticles (MNPs) [17]. Subramanian *et al.* [14] demonstrated the advantages of using hyperthermia in a neuroblastoma cell line in-vitro as opposed to relying solely on the toxic effects of FDG-MNP's. In our study, we present further data concerning the toxic effects of FDG-MNP with and without the application of hyperthermia to NIC-H727 cancer cells.

Wang *et al*. [18] developed MNPs which helped in the detection of micro metastasis in lung cancer. The cytokeratin's are abundantly expressed in metastatic epithelial tumours. This expression facilitates the typing of normal, metaplastic, and neoplastic cells. Recognition of this expression in NSCLC helps in detecting the metastatic lung cancer cells from other cells. Wang *et al*. reported the conjugation of MNPS with pan-cytokeratin helps in isolating circulating cancer cell in NSCLC patient [18]. This type of findings might assist the selective cellular uptake of drug loaded MNPs tagged with pan-cytokeratin for the cell specific delivery of chemotherapeutic agents.

Fluorodeoxyglucose conjugated MNPs (FDG-MNPs) have recently been shown to be effective in the targeting of neuroblastomas [13]. The conjugation of these MNPs to the glucose analogue fluorodeoxyglucose (FDG) is thought to improve cellular MNP incorporation and induce cytotoxicity in cancer cell lines. It is well known that cancer cells have a great affinity for the uptake of glucose; The Warburg effect [19, 20]. Since FDG is a glucose analogue, it is believed that it is rapidly taken up by cancer cells. This has been shown by some reports [14, 15].

In human lung cancer, iron oxide nanoparticles alone are known to induce membrane damage and apoptosis of A549 cancer cells [15]. It is therefore important to determine whether FDG coupled with iron oxide magnetic nanoparticles can exert the same destructive effect on human lung cancer cells.

Experimental

Synthesis and Characterization of MNPs and FDG-MNPs

MNPs were synthesized, coated in silica, and fabricated with TEOS (tetraethyl orthosilicate). These modified MNPs were then conjugated with [^{19}F]FDG, optically labelled with ICG (indocyanine green) and characterized similarly as described in our previous reports [8, 10, 12, 21].

The hydrodynamic diameter of the FDG-MNPs was measured using a dynamic light scattering device (Malvern Nano ZS DLS, Malvern, UK). For that the MNPs or FDG-MNPs were dispersed in 20% dextrose solution at FDG-MNP (100 μg.mL^{-1}) concentration and measured at 25 °C. Measurements were repeated three times, and the results were expressed as the mean ± standard deviation. Particle size and morphology of the synthesized MNPs were obtained using scanning electron microscopy (SEM) (Thermo Fisher Scientific QUANTA 250, FEG, Massachusetts, USA). Structural analyses of MNPs, silica-coated MNPs, silane-coupled MNPs, and FDG-MNPs was conducted with a Perkin-Elmer Spectrum Two Fourier-Transform Infrared Spectroscopy (FT-IR) spectrometer (Massachusetts, USA) using the Attenuated Total Reflection method.

Iron concentration was measured using an Inductively Coupled Plasma and Mass Spectrometry (ICP-MS) (Agilent Technologies 7900 ICP-MS SPS4 Auto sampler, California, USA).

Toxicity tests

Two initial tests were performed, hereafter referred to as the minimum toxicity test and the exposure test. The toxicity test involved the absorption of MNPs (magnetic nanoparticles) into cells and subsequent dead cell counting after 24 hours; the exposed test had no absorbance time (t=0). The field exposure time was 5 minutes, after which cell death was counted.

Maximum toxicity testing at higher concentrations of MNPs showed the percentage cell death initially, and over a period of time. The purpose of these tests was to determine any differences in cell death when MNPs were used in conjunction with and without a magnetic field. We also assessed the extent of cell death expected at different MNP concentrations. Details of the NIC-H727 cancer cell line used and setting up of the cancer cells wells are given in appendices 1 and 2. NCI-H727 cells were used at passage 14, 15, and 16 (Graphical abstract).

Minimum toxicity test

A 24-well plate was seeded and allowed to grow in RPMI 1640 media (Sigma-Aldrich) overnight. On the day of testing, a confluency of 95% was noted. Consequently, approximately $1.9x10^5$ cells were estimated to be in each well (ThermoFisherScientific, 2018) [22]. All media was removed from wells, and fresh media mixed with MNPs was added to each well. Six different concentrations of MNPs were used in quadruplicate: 0.006 mg/mL, 0.012 mg/mL, 0.024 mg/mL, 0.048 mg/mL, 0.06 mg/mL, and 0.12 mg/mL. These concentrations were created by diluting the initial concentration of MNPs in the media before adding to each well. The final solution in each well totalled 400 uL (0.4 mL). After an incubation period of 24 h at 37 °C, dead cells were counted in trypan blue. At least 3 counts were performed in each grid, and 2 for each concentration (total of 6 separate counts for each well). The cell suspension was taken directly from the well, without disturbing the live cells attached to the bottom of the well. An average cell count was established and mathematically scaled up to give a representative number of dead cells per volume of liquid in the well. This number is then given as a percentage of the original $1.9x10^5$ cells expected to be in each well.

Exposure test

A 6-well plate was seeded and allowed to grow in RPMI media overnight. On the day of testing, a confluency of 40% was noted. Consequently, approximately $4.8x10^5$ cells were estimated to be in each well. Again, all media was removed and a solution of fresh media and MNPs was created for each well, totalling 1.5 mL. Six different concentrations of MNPs were used, across the six wells: 0 mg/mL, 0.006 mg/mL, 0.012 mg/mL, 0.024 mg/mL, 0.048 mg/mL, and 0.06 mg/mL. The six solutions were not added until immediately before exposure to the field, to allow no absorption time. 1 mL of media was added to keep the cells covered, and the media with MNPs was added directly before exposure. Approximately 40 s passed between addition of the MNPs and beginning of the field exposure. The well was subjected to a 5-min exposure time at 480.4 kHz and 72 V. After this, cells were again counted in trypan blue. Counting was replicated (totalling 6 counts for each grid) and an average taken and scaled up. This number is

given as a percentage of the original $4.8x10^5$ cells.

Maximum toxicity test

Stock cells from a T75 flask were passaged and resuspended in a small volume of RPMI 1640 media (volume varied from 1-5 mL). A very small volume of media was required to achieve a high number of cells (facilitating easier and more accurate counting). Cells in the suspension were counted prior to seeding, and then 100 µL was added to six wells. Cells were not allowed to grow overnight and were tested immediately. Six different 50 µL dilutions of PBS and MNPs were created, resulting in the following MNP concentrations: 0 mg/mL, 0.21 mg/mL, 0.3 mg/mL, 0.42 mg/mL, 0.51 mg/mL, and 0.6 mg/mL. These solutions were added to the wells containing cells and media, mixed thoroughly by pipetting, and the cells counted in trypan blue. This cell count is described as t0 (time=0 h). Each cell count was repeated up to four times and averages were calculated. Cells were also counted at t2 (time=2 h) and t24 (time=24 h). During the time between counting, the plates were stored in an incubator at 37 °C.

EC50 (measure for potency) values were assessed for cytotoxicity profile. Statistical analysis including ANOVA was done using inbuilt add-in of the Graph Pad Program.

Results and Discussion

Structural properties of MNPs and FDG-MNPs

The nanoparticles were homogeneously dispersed in dextrose (80% water, 20% dextrose) solution according to Dynamic Light Scattering measurement. The medium size was 176.7±4.7 nm (n=5) together with their hydrodynamic radius (Figure 1). The surface potential of MNPs and FDG-MNPs were found to be −4.77 ± 0.918 mV and 21.26 ± 0.862 mV respectively. Increasing the surface potential at a physiologically relevant pH 7.4 suggests good colloidal stability of the FDG MNPs. SEM data showed that FDG-MNPs possessed a particle shape that was a uniform homogeneous structure, with a particle size of around 20-30 nm (Figure 2). The FT-IR spectra confirmed the peaks at around 3369 cm^{-1} from O–H stretching and 550 cm^{-1} from the Fe–O band of MNPs (Figure 3). Results are agree with our previous data [8, 10, 14, 21].

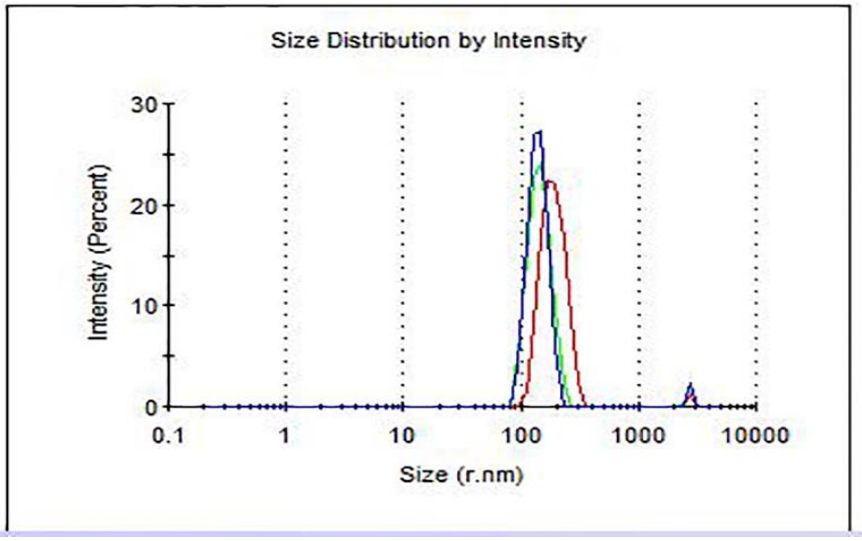

Figure 1. Dynamic light scattering spectra of the FDG-MNPs

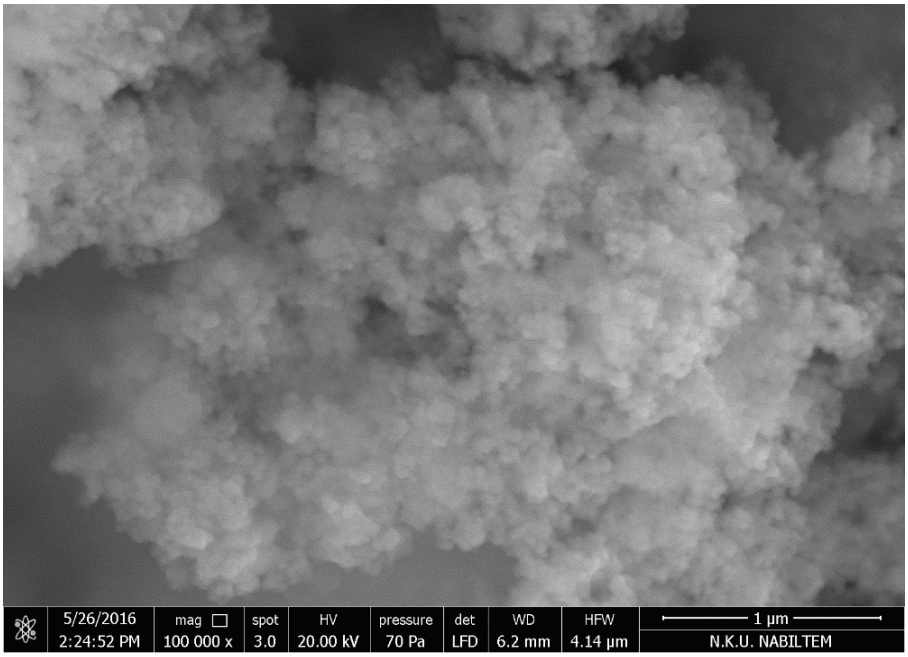

Figure 2. SEM Image of FDG-MNPs

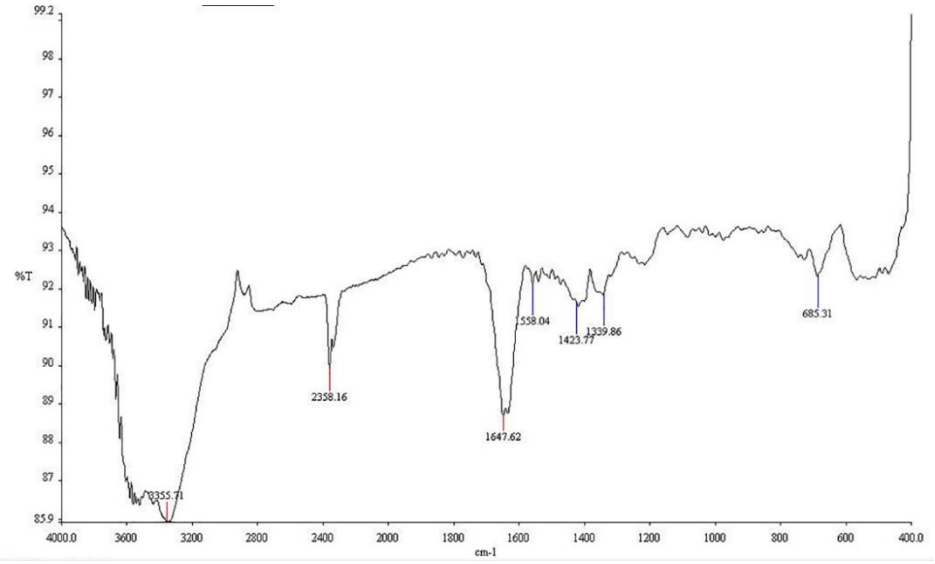

Figure 3. Fourier transform infrared spectra (FTIR) of FDG-MNPs

Minimum toxicity and exposure test

It was discovered that the percentage cell death was much higher in the presence of the magnetic field, as demonstrated in Figure 4. Toxicity of MNPs is shown by the percentage cell death caused by five different concentrations (A) and over a period of three time points (B) (see Graphical abstract).

The difference between lines is even more significant since an increased absorbance time is expected to cause more cell death. Since the toxicity line showed 24 hours of absorbance and the field exposure line indicated 0-hour absorbance, this shows that the field increases

cell death more than using MNPs alone, and more than with using MNPs with a very long absorbance time.

The results indicate that the magnetic field was able to destroy cells containing MNPs, while MNPs alone had significantly lower effects. It also suggests that MNPs alone in these low concentrations would have little adverse effects on healthy (non-target) cells.

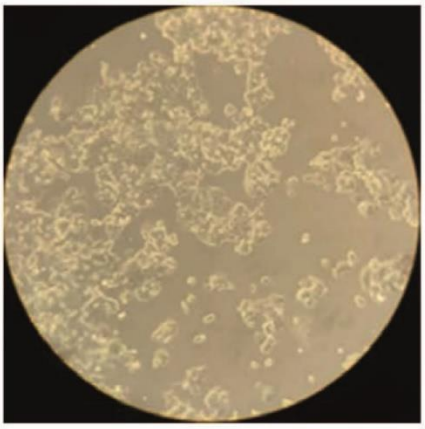

Dilution	0.01	0.02	0.04	0.08	0.1	0.2
Concentration	0.006	0.012	0.024	0.048	0.06	0.12
Volume mNP (µL)	4	8	16	32	40	80
Volume Media (µL)	396	392	384	368	360	320

Figure 4. Toxicity test of FDG-MNP-ICG. (The table shows the concentrations and volumes for each well)

The cell counts at t0 revealed that cell death increased in a linear fashion, with increasing concentration of MNPs. When the absorbance time of MNPs was increased, the cell death also rose significantly (Figure 5). The MNPs were left in the wells during this time, and no new media was added. At t2 and t24, the percentage cell death was not corrected for the number of cells that died without any MNP involvement, and so the actual cell death may have been lower than that shown. 50% cell death was achieved around 0.6 mg/mL for t0, but at 0.3 mg/mL for higher absorbance times. EC50s (effective concentrations) and IC50s (inhibitory concentrations) are used early in the process to evaluate the suitability and the performance of the agents [23]. EC50 values were estimated by Graph Pad. Iron oxide nanoparticles (MNPs) have been employed in several biomedical applications where they facilitate both diagnostic and therapeutic aims. Although the potential benefits of MNPs with different surface chemistry and conjugated targeting ligands/proteins are considerable, complicated interactions between these nanoparticles (NPs) and cells leading to toxic impacts could limit their clinical applications [24].

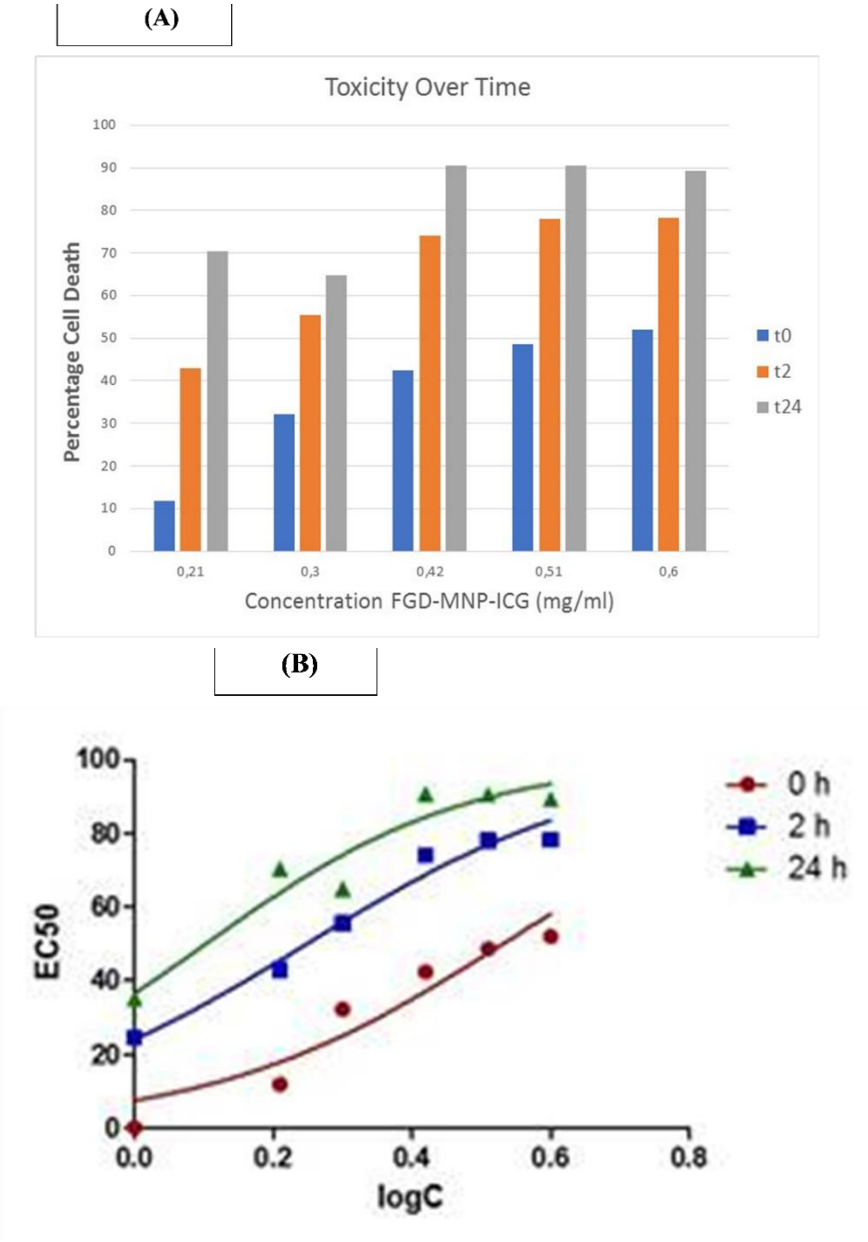

Figure 5. a) Dose-response curve of MNPs shown by the percentage cell death caused by five different concentrations and b) cytotoxicity plot ± SD of same agents on noncancerous cell NIC-H727 human lung, bronchus epithelial cells (EC50) over a period of three time points

For cells in tissues or animals, it is more likely that less cells will die from MNP toxicity, and longer absorbance times may be required. Iron oxide nanoparticles have been combined with many drug molecules to increase the anticancer potential in targeted drug applications [25]. Performing toxicity studies with in-vitro methods is an important step in examining the toxicity and effectiveness of these nanocomposites. A number of nanoparticles and conventional/herbal medicine conjugates have been developed to increase anticancer performance and reduce side effects. Recently, few techniques based on various MNP designs have been applied in the field of tumour therapy: magnetic hyperthermia

(MHT) [26, 27], photodynamic therapy (PDT) [28, 29], and photothermal therapy [30]. In parallel with their increasing use for biomedical applications, safety concerns on human organisms have also increased [31, 32]. Moreover, investigating accumulation of FDG-MNPs in cell cultures and *in-vivo*, reveals insight into their effects on such factors as proliferation, viability, toxicity, and such studies are of paramount importance in terms of their clinical activity [33, 34].

Our results indicated that the magnetic field was able to destroy cells with MNPs, but MNPs alone have significantly lower effects. The results also suggested that MNPs alone in these low concentrations would have little adverse effects on healthy (non-target) cells. However, previous studies have shown that FDG-MNP's in high concentrations do have toxic effects on cancer cells when used alone without the application hyperthermia [8].

In future studies, rather than investigating the action of MNP concentration on cells, it may be beneficial to work in micrograms of MNPs per cell. This may provide more realistic values regarding the dosage needed for a patient and enable comparisons with studies using different organizations of cells; in-vitro, in-vivo tissues and animals.

Future experiments could test even higher concentrations of MNPs, using methods described here or in previous reports, which discuss MNP factors such as the absorption into cells, removal, and the addition of fresh media before counting [14].

Conclusions

This report presents data involving NIC-H727 human lung, bronchus epithelial cells exposed to conjugated fluorodeoxyglucose conjugated with iron-oxide magnetic nanoparticles and indocyanine green (ICG) dye (FDG-MNP-ICG), with and without the application of a magnetic field. Magnetic field was able to destroy cells with MNPs, but MNPs alone have significantly lower effects. MNPs alone in these low concentrations would have little adverse effects on non-target cells. As conclusion FDG-MNP's may have uses as a potential cancer therapy with magnetic hyperthermia in clinical applications.

Acknowledgements

Authors would like to appreciate the NIH/NCI Cancer Support Grant P30 CA008748 and the manuscript approved by Internal Review Board.

Disclosure Statement

No potential conflict of interest was reported by the authors.

Orcid

Perihan Unak 0000-0002-5464-2987

Rachel Hepton 0000-0002-5572-4802

Max Harper 0000-0003-1783-5103

Volkan Yasakci 0000-0002-4133-3886

Gillian Pearce 0000-0003-1428-2021

Steve Russell 0000-0002-5491-900X

Oguz Akin 0000-0002-2041-6199

Julian Wong 0000-0002-9708-9077

References

[1]. Ferlay J., Steliarova-Foucher E., Lortet-Tieulent J., Rosso S., Coebergh J.W.W., Comber H., Forman D., Bray F. *Eur J Cancer*, 2013, **49:**1374

[2]. Siegel R.L., Miller K.D., Jemal A. *CA Cancer J Clin*, 2019, **69:**342019

[3]. Bray F., Ferlay J., Soerjomataram I., Siegel R.L., TorreL A., Jemal A. *CA Cancer J Clin*., 2018, **68**:394

[4]. Ferlay J., Shin H.R., Bray F., Forman D., Mathers C., Parkin D.M. *Int J Cancer*, 2010, **127**:2893

[5]. Jabir N.R., Tabrez S., Ashraf G.M., Shakil S. *Int. J. Nanomed*., 2012, **7**:4391

[6]. Shubayev V.I., Pisanic T.R., Jin S. *Adv. Drug Deliv. Rev.,* 2009, **61**:467

[7]. Qiao H., Liu W., Gu H., Wang D., Wang Y., *J. Nanomater*., 2015, **8**:394507

[8]. Aras O., Pearce G., Watkins A.J., Nurili F., Medine E.I., Guldu O.K., Tekin V., Wong J., Ma X., Ting R., Unak P. *PloS one*, 2018, **13**:e0202482

[9]. Huang H.S., Hainfeld J.F. *Int. J. Nanomed*., 2013, **8**:2521

[10]. Ozkaya F., Unak P., Medine E.I., Sakarya S., Unak G., Timur S. *J. Radioanal. Nucl. Chem.,* 2013, **295**:789

[11]. Veiseh O., Gunn J.W., Zhang M. *Adv. Drug Del. Rev*., 2010, **62**:284

[12]. Watkins A.J., Pearce G., Unak P., Guldu O.K., YasakciV., Akin O., Aras O., Wong J., Ma X. *J. Biomed. Nanotech*., 2018, **14:**1979

[13]. Attar M.M., Haghpanahi M. *Electromag. Biol. Med*., 2016, **35**:305

[14]. Subramanian M., Pearce G., Guldu O.K., Tekin V., Miaskowski A., Aras O., Unak P. *IEEE Trans. Nanobio*., 2016, **15**:517

[15]. Atkinson W.J., Brezovich I.A., Chakraborty D.P. *IEEE Trans. Biomed. Eng.,* 1984, **31**:70

[16]. Creixell M., Bohorquez A.C., Torres-Lugo M., Rinaldi C. *ACS Nano*, 2011, **5**:7124

[17]. Choi S.J., Oh J.M., Choy J.H. *J. Inorg. Biochem*., 2009, **103**:463

[18]. Wang Y., Zhang Y., Du Z., Wu M., Zhang G. *Int. J. Nanomed.,* 2012, **7**:2315

[19]. Park S.G., Lee J.H., Lee W.A., Han K.M. *Nucl.Med. Biol.*, 2012, **39**:1167

[20]. San-Millán I., Brooks G.A. *Carcinogenesis*, 2017, **38**:119

[21]. Unak P., Budiyo R., Horsnzky A., Yasakci V., Pearce G., Russell S., Aras O., Oguz A., Wong J. *Asian Journal of Nanosciences and Materials*, 2021, **4:**53

[22]. Vítová M., Hendrychová J., Cepák V., Zachleder V. *Folia Microbiol (Praha),* 2005, **50**:333

[23]. Sebaugh J. L. *Pharm Stat*., 2011, **10**:128

[24]. Vakili-Ghartavol R., Momtazi-Borojeni A.A., Vakili-Ghartavol Z., Aiyelabegan H.T., Jaafari M.R., Rezayat S.M., Bidgoli S.A. *Art. Cells, Nanomed. Biotech*., 2020, **48**:443

[25]. Ramazanov M., Karimova A., Shirinova H. *Biointerface Res. Appl.Chem*., 2021, **11**:8654

[26]. Yin P.T., Shah B. P., Lee K.B. *Small*, 2014, **10**:4106

[27]. Jose J., Kumar R., Harilal S., Mathew G.E., Parambi D.G.T., Prabhu A., Uddin M.S., Aleya L., Kim H., Mathew B. *Environ. Sci. Poll. Res*., 2020, **27:**19214

[28]. Agostinis P., Berg K., Cengel K.A., Foster T.H., Girotti A.W., Gollnick S.O., Hahn S.M., Hamblin M.R., Juzeniene A., Kessel D., Korbelik M., Moan J., Mroz P.; Nowis D., Piette J., Wilson B.C., Golab J. *CA: Cancer J. Clin*., 2011, **61**:250

[29]. Janko C., Ratschker T., Nguyen K., Zschiesche L., Tietze R., Lyer S., Alexiou C. *Front Oncol*., 2019, **9**:59

[30]. J. Estelrich, M.A. Busquets, *Molecules*, 2018, **23:**1567

[31]. Wang C., Bao C., Liang S., Zhang L., Fu H., Wang Y., Wang K., Li C., Deng M., Liao Q., Ni J.; Cui D. *Nanoscale Res. Lett*., 2014, **9**:274

[32]. Mahmoudi M.,.Hofmann H., Rothen-Rutishauser B., Petri-Fink A. *Chem. Rev.,* 2012, **112**:2323

[33]. Thorat N.D., Shinde K.P., Pawar S.H., Barick K.C., Betty C.A., Ningthoujam R.S. *Dalton Trans*., 2012, **41**,3060

[34]. Thorat N.D., Bohara R.A., Noor M.R., Dhamecha D., Soulimane T., Tofail S.A.M. *ACS Biomat. Sci. Engin*., 2017, **3**:1332

How to cite this manuscript: Perihan Unak*, Rachel Hepton, Max Harper, Volkan Yasakci, Gillian Pearce, Steve Russell, Omer Aras, Oguz Akin, Julian Wong. Toxicity testing of indocyanine green and fluorodeoxyglucose conjugated iron oxide nanoparticles with and without exposure to a magnetic field. *Asian Journal of Nanoscience and Materials*, 4(3) 2021, 229-239. DOI: 1026655/AJNANOMAT.2021.3.5